SCIENTIFIC REPORTS

OPEN

Anomalous incident-angle and elliptical-polarization rotation of an elastically refracted P-wave

Received: 11 March 2015
Accepted: 07 July 2015
Published: 05 August 2015

Lin Fa[1], Yuxiao Fa[2], Yandong Zhang[1], Pengfei Ding[1], Jiamin Gong[1], Guohui Li[1], Lijun Li[1], Shaojie Tang[1] & Meishan Zhao[3]

We report a newly discovered anomalous incident-angle of an elastically refracted P-wave, arising from a P-wave impinging on an interface between two VTI media with strong anisotropy. This anomalous incident-angle is found to be located in the post-critical incident-angle region corresponding to a refracted P-wave. Invoking Snell's law for a refracted P-wave provides two distinctive solutions before and after the anomalous incident-angle. For an inhomogeneously refracted and elliptically polarized P-wave at the anomalous incident-angle, its rotational direction experiences an acute variation, from left-hand elliptical to right-hand elliptical polarization. The new findings provide us an enhanced understanding of acoustical-wave scattering and lead potentially to widespread and novel applications.

Concerning the interior of the Earth, it is a common understanding that the interior is composed of the regular sequences of isotropic thin layers of different properties. When the prevailing wavelength of a seismic wave is larger than the thickness of the individual layers, the sequences of thin layers behave anisotropically, whereas still transversely isotropic[1–4]. This macroscopically transversely isotropic medium with a vertical axis of symmetry is called a VTI medium[5]. In such a case, the mechanical property of a VTI medium can be described by the elastic stiffness tensor of a hexagonal crystal[3–7]. Based on these understandings, the influences of rock anisotropy on polarization, propagation and reflection/refraction of elastic waves have been studied and reported extensively[7–12], e.g. the polarization direction of an elastic P-wave, which is different from propagation direction; the propagation velocity that is different from phase velocity; and the reflection/refraction coefficients, which vary with respect to the acoustic impendence and anisotropy of media.

The study on reflection of acoustic wave is very important to geophysics; for example, Nedimovic *et al.* analyzed the reflection signature of seismic and aseismic slip on the northern Cascadia subduction interface[13] and Canales *et al.* discussed the seismic reflection images of a near-axis sill within the lower crust of the Juan de Fuca ridge[14]. Acoustic waves also bear many similarities to optical or electromagnetic waves in propagation, reflection, refraction, and polarization. Grady *et al.* reported linear conversion and anomalous refraction for electromagnetic waves[15]. Genevet *et al.* studied the phenomena of anomalous reflection/refraction of light and its propagation with phase discontinuities[16]. Fa *et al.* predicted the existence of an anomalous incident-angle for an inhomogeneously refracted P-wave[11].

In this paper, we show that there exists a physically significant anomalous incident-angle for the refracted P-wave. With this anomalous incident-angle, the incident-angle region can be classified into three sections: the pre-critical incident-angle region, the area between the critical incident-angle and the anomalous incident-angle, and the post-anomalous incident-angle region. There are two distinctive phase velocity solutions before and after the anomalous incident-angle. For an inhomogeneously refracted

[1]School of Electronic Engineering, Xi'an University of Posts and Telecommunications, Xi'an, Shaanxi 710121, China. [2]Kunlun Energy Company Limited, Hongkong 999077, China. [3]James Franck Institute and Department of Chemistry, The University of Chicago, Chicago, IL 60637, USA. Correspondence and requests for materials should be addressed to L.F. (email: faxiaoxue@126.com or fa_yy@aliyun.com)

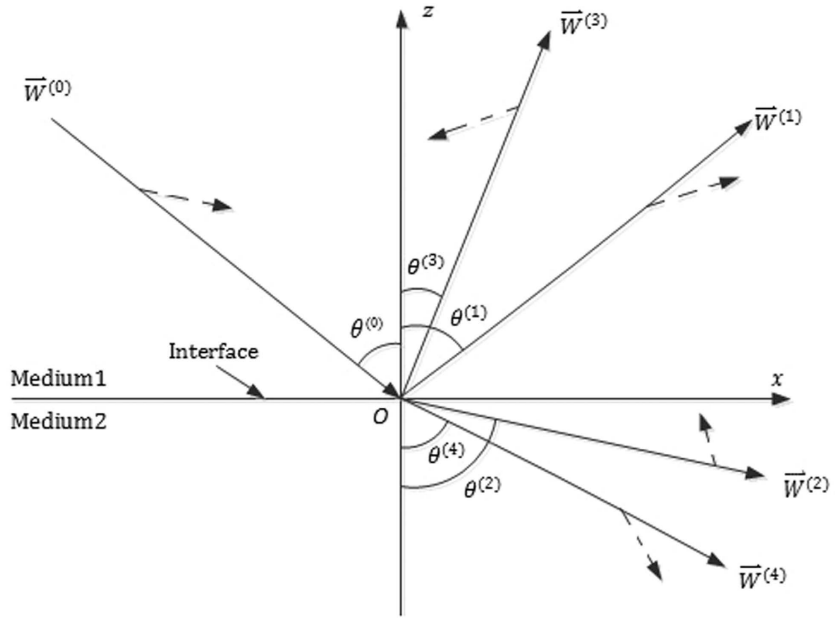

Figure 1. Polarization vector and wave-front normal for incident P-wave and induced waves at the interface. The solid-lines with arrowhead indicate the phase velocity direction and the dashed-lines with arrowhead show the polarization direction; $\overrightarrow{W}^{(m)}$ is a displacement and $m = \{0, 1, 2, 3, 4\}$ denotes the incident P-wave, reflected P-wave, refracted P-wave, reflected SV-wave and refracted SV-wave, respectively.

Medium	$\alpha^{(n)}$ (m/s)	$\beta^{(n)}$ (m/s)	$\rho^{(n)}$ (g/cm^3)	Thomsen Parameters			Elastic constants (GPa)				
				$\varepsilon^{(n)}$	$\delta^{*(n)}$	$\gamma^{(n)}$	C_{11}	$C_{13}^{(n)}$	$C_{33}^{(n)}$	$C_{44}^{(n)}$	$C_{66}^{(n)}$
A-shale	2745	1508	2.340	0.103	−0.073	0.345	21.264	6.976	17.632	5.321	8.993
O-shale	4231	2539	2.370	0.200	0.000	0.145	9.397	15.824	42.426	15.278	19.709

Table 1. Anisotropic parameters and elastic constants for A-shale and O-shale. The superscript $n = \{in, re\}$ donates the incidence medium and refraction medium.

elliptically-polarized P-wave, the anomalous incident-angle will cause an acute rotational-direction variation.

Results

Modeling. Considering a P-wave propagating in the x-z plane impinging on the interface (x-y plane) between two VTI media, the system can be described schematically as in Fig. 1.

We performed calculations for two sedimentary rocks with some very well-known physical properties, as reported by geophysicists and given in Table 1 [2,11,17]. In this paper, we use anisotropic shale (A-shale) as the incidence medium and oil shale (O-shale) as the refraction medium. For this system, by calculation, we found that there is an anomalous incident-angle at $\theta_a^{(2)} = 62.04^\circ$.

The elements of the elastic stiffness tensor, related to the anisotropic rock parameters, are given by Thomsen[2],

$$c_{13}^{(n)} = \rho^{(n)}\sqrt{[\delta^{*(n)}(\alpha^{(n)})^4] + \left[(\alpha^{(n)})^2 - (\beta^{(n)})_v^2\right]\left[(\varepsilon^{(n)} + 1)(\alpha^{(n)})^2 - (\beta^{(n)})^2\right]} - \rho^{(n)}(\beta^{(n)})^2, \quad (1)$$

$$c_{33}^{(n)} = \rho^{(n)}(\alpha^{(n)})^2, \quad (2)$$

$$c_{11}^{(n)} = [2\varepsilon^{(n)} + 1]\rho^{(n)}[\alpha^{(n)}]^2, \quad (3)$$

$$c_{44}^{(n)} = \rho^{(n)}(\beta^{(n)})^2, \quad (4)$$

$$c_{66}^{(n)} = [2\gamma^{(n)} + 1]\rho^{(n)}(\beta^{(n)})^2, \tag{5}$$

For a harmonic acoustic-field, the wave displacements $\overrightarrow{W}^{(m)}$ can be written as

$$\overrightarrow{W}^{(0)} = R^{(0)}\begin{pmatrix} u_x^{(0)} \\ -u_z^{(0)} \end{pmatrix}\exp\{i[\omega t - k^{(0)}x\ \sin\ \theta^{(0)} + k^{(0)}z\ \cos\ \theta^{(0)}]\}, \tag{6}$$

$$\overrightarrow{W}^{(1)} = |R^{(1)}|\begin{pmatrix} u_x^{(1)} \\ u_z^{(1)} \end{pmatrix}\exp\{i[\omega t - k^{(1)}x\ \sin\ \theta^{(1)} - k^{(1)}z\ \cos\ \theta^{(1)} + \phi^{(1)}]\}, \tag{7}$$

$$\overrightarrow{W}^{(2)} = |R^{(2)}|\begin{pmatrix} u_x^{(2)} \\ -u_z^{(2)} \end{pmatrix}\exp\{i[\omega t - k^{(2)}x\ \sin\ \theta^{(2)} + k^{(2)}z\ \cos\ \theta^{(2)} + \phi^{(2)}]\}, \tag{8}$$

$$\overrightarrow{W}^{(3)} = |R^{(3)}|\begin{pmatrix} -u_z^{(3)} \\ -u_x^{(3)} \end{pmatrix}\exp\{i[\omega t - k^{(3)}x\ \sin\ \theta^{(3)} - k^{(3)}z\ \cos\ \theta^{(3)} + \phi^{(3)}]\}, \tag{9}$$

$$\overrightarrow{W}^{(4)} = |R^{(4)}|\begin{pmatrix} -u_z^{(4)} \\ u_x^{(4)} \end{pmatrix}\exp\{i[\omega t - k^{(4)}x\ \sin\ \theta^{(4)} + k^{(4)}z\ \cos\ \theta^{(4)} + \phi^{(4)}]\}. \tag{10}$$

In the equations above, $\theta^{(m)}$ is either an incident-angle or a reflection/refraction angle, and $u_x^{(m)}$ and $u_z^{(m)}$ are polarization coefficients; $\phi^{(m)}$ is the phase shift for an induced wave relative to the incident P-wave and $\phi^{(0)}$ is defined as 0°; $R^{(m)}$ is either the reflection or refraction coefficient for each induced wave, and $R^{(0)}$ is defined as 1. For the refracted P-wave, the critical incident-angle is denoted by $\theta_c^{(2)}$, and the anomalous incident-angle is given as $\theta_a^{(2)}$.

For the incident-angle range of $\theta^{(0)} < \theta_c^{(2)}$, the reflection/refraction coefficients are real (not complex) and $\phi^{(m)}$ is 0° or 180°. In the range of $\theta^{(0)} > \theta_c^{(2)}$, the reflection/refraction coefficients are complex and $\phi^{(m)} \in (-180°, 180°)$.

Verification of an anomalous incident-angle. The core existence of an anomalous incident-angle for an elastically refracted P-wave can be confirmed from Snell's law. Based on the Christoffel equation, the solutions of the phase velocity for the incident wave (P-wave or SV-wave) and the four induced waves are given by[3,8]

$$v_{1,2}^{(m)} = \frac{\sqrt{2}}{2}\sqrt{A_4^{(n)} + A_5^{(n)}\sin^2\theta^{(m)} \pm \sqrt{2A_1^{(n)}\sin^2\theta^{(m)} + A_2^{(n)}\sin^4\theta^{(m)} + A_3^{(n)}}}, \tag{11}$$

where $A_1^{(n)} = 2(A_{13}^{(n)} + A_{44}^{(n)})^2 - (A_{33}^{(n)} - A_{44}^{(n)})(A_{11}^{(n)} + A_{33}^{(n)} - 2A_{44}^{(n)})$, $A_2^{(n)} = (A_{11}^{(n)} + A_{33}^{(n)} - 2A_{44}^{(n)})^2 - 4(A_{13}^{(n)} + A_{44}^{(n)})^2$, $A_3^{(n)} = (A_{33}^{(n)} - A_{44}^{(n)})^2$, $A_4^{(n)} = A_{33}^{(n)} + A_{44}^{(n)}$, $A_5^{(n)} = A_{11}^{(n)} - A_{33}^{(n)}$. Denoting the anomalous incident-angle as $\theta_a^{(2)} \in (\theta_c^{(2)}, 90°)$, the phase velocities of the refracted P-wave are $v_1^{(2)}$ for $\theta^{(0)} \in [0°, \theta_a^{(2)}]$ and $v_2^{(2)}$ for $\theta^{(0)} \in [\theta_a^{(2)}, 90°]$. They abide by Snell's law such that $\sin\ \theta^{(2)}/v_1^{(2)} = \sin\ \theta^{(0)}/v_1^{(0)}$ for $\theta^{(0)} \in [0°, \theta_a^{(2)}]$, and $\sin\ \theta^{(2)}/v_2^{(2)} = \sin\ \theta^{(0)}/v_1^{(0)}$ for $\theta^{(0)} \in [\theta_a^{(2)}, 90°]$.

The reflection/refraction angles are calculated from the fourth-order polynomials of $\sin\ \theta^{(m)}$[11]

$$B_1^{(in)}(\theta^{(0)})\sin^4\theta^{(1,3)} + B_3^{(in)}(\theta^{(0)})\sin^2\theta^{(1,3)} + B_5^{(in)} = 0, \tag{12}$$

$$B_1^{(re)}(\theta^{(0)})\sin^4\theta^{(2,4)} + B_3^{(re)}(\theta^{(0)})\sin^2\theta^{(2,4)} + B_5^{(re)} = 0 \tag{13}$$

where, $B_1^{(in)}(\theta^{(0)}) = A_2^{(in)} - [K_1(\theta^{(0)})]^2$, $B_3^{(in)}(\theta^{(0)}) = 2[A_1^{(in)} - A_4^{(in)}K_1(\theta^{(0)})]$, $B_5^{(in)} = A_3^{(in)} - [A_4^{(in)}]^2$, $B_1^{(re)}(\theta^{(0)}) = A_2^{(re)} - [K_2(\theta^{(0)})]^2$, $B_3^{(re)}(\theta^{(0)}) = 2[A_1^{(re)} - A_4^{(re)}K_2(\theta^{(0)})]$, $B_5^{(re)} = A_3^{(re)} - [A_4^{(re)}]^2$, $K_1(\theta^{(0)}) = 2/const\,(\theta^{(0)}) - A_4^{(in)}$, $K_2(\theta^{(0)}) = 2/const\,(\theta^{(0)}) - A_4^{(re)}$, and $const\,(\theta^{(0)}) = [\sin\ \theta^{(0)}/v_1^{(0)}]^2$. Eq. (13) can be used to calculate the refraction angles and determine the existence of the anomalous incident-angle, denoted by $\theta_a^{(2)}$.

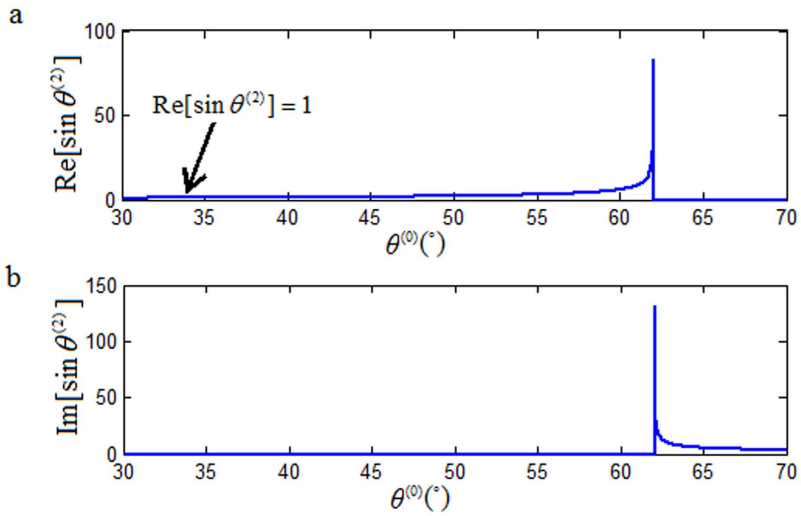

Figure 2. Relationship between $\sin\theta^{(2)}$ and $\theta^{(0)}$. (**a**) For $\theta^{(0)} \in [0^\circ, \theta_a^{(2)}]$, $\sin\ \theta^{(2)}$ is purely real. (**b**) For $\theta^{(0)} \in [\theta_a^{(2)}, 90^\circ]$, $sin\,\theta^{(2)}$ is purely imaginary. There is an obvious abnormality provided at $\theta_a^{(2)} = 62.04^\circ$.

As shown in Fig. 2a, the value of $\sin\ \theta^{(2)}$ is purely real for $\theta^{(0)} \in [0^\circ, \theta_a^{(2)}]$; whereas for $\theta^{(0)} \in [\theta_a^{(2)}, 90^\circ]$, it is purely imaginary, as shown in Fig. 2b. Figure 3a,b show that for $\theta^{(0)} \in [0°, 90°]$, $v_1^{(2)}$ is real (not complex). In Fig. 3c,d, the value of $v_2^{(2)}$ is real for $\theta^{(0)} \in [0^\circ, 46.61^\circ]$ and purely imaginary for $\theta^{(0)} \in [46.61^\circ, 90^\circ]$. For $\theta^{(0)} \in [62.04^\circ, 90^\circ]$, both $\sin\ \theta^{(2)}$ and $v_2^{(2)}$ are purely imaginary. Figure 4b,c show that $\sin\ \theta^{(2)}/v_1^{(2)}$ is equal to $\sin\ \theta^{(0)}/v_1^{(0)}$ for $\theta^{(0)} \in [0^\circ, 62.04^\circ]$ and $\sin\ \theta^{(2)}/v_2^{(2)}$ is equal to $\sin\ \theta^{(0)}/v_1^{(0)}$ for $\theta^{(0)} \in [62.04^\circ, 90^\circ]$. The curve segment $\overline{AB}$ in Fig. 4b plus curve segment $\overline{CD}$ in Fig. 4c forms the curve in Fig. 4d, which is the same as that in Fig. 4a. Here, for $\theta^{(0)} \in [46.61^\circ, 62.04^\circ]$, $\sin\ \theta^{(2)}$ is purely real and $v_2^{(2)}$ is purely imaginary, so during the plotting of the relationship of $\sin\ \theta^{(2)}/v_2^{(2)}$ versus $\theta^{(0)}$, the computer takes the value of $\sin\ \theta^{(2)}/v_2^{(2)}$ as zero automatically.

These results show clearly that Snell's law is satisfied only if the phase velocity solution of the refracted P-wave is switched to $v_2^{(2)}$ from $v_1^{(2)}$ at $\theta^{(0)} = 62.04°$. And therefore, there is an anomalous incident-angle of $\theta_a^{(2)} = 62.04^\circ$. It resides in a region passing the critical incident angle $\theta_c^{(2)} = 33.65^\circ$, up to an incident angle 90°.

Verification of elliptically-polarized rotational direction change. Verification of elliptically-polarized rotational direction change can be achieved by invoking the so called energy balance principle. The polarization coefficients for the incident wave and the four induced waves are given by[11]

$$(u_x^{(m)})^* u_z^{(m)} = -\frac{\Gamma_{13}^{(m)}(\Gamma_{13}^{(m)})^*}{(\Gamma_{13}^{(m)})^*\left[\Gamma_{33}^{(m)} - \left(v_{1,2}^{(m)}\right)^2\right] + \Gamma_{13}^{(m)}\left[\Gamma_{11}^{(m)} - \left(v_{1,2}^{(m)}\right)^2\right]^*}, \tag{14}$$

and

$$u_x^{(m)}(u_z^{(m)})^* = -\frac{\Gamma_{13}^{(m)}(\Gamma_{13}^{(m)})^*}{\Gamma_{13}^{(m)}\left[\Gamma_{33}^{(m)} - \left(v_{1,2}^{(m)}\right)^2\right]^* + (\Gamma_{13}^{(m)})^*\left[\Gamma_{11}^{(m)} - \left(v_{1,2}^{(m)}\right)^2\right]}, \tag{15}$$

where the definitions of $\Gamma_{11}^{(m)}$, $\Gamma_{13}^{(m)}$ and $\Gamma_{33}^{(m)}$ refer to those of Eq. (S2) in "Supplementary material for Anomalous incident-angle and elliptical-polarization rotation of an elastically refracted P-wave".

From Eqs. (14) and (15) we can obtain the expressions of polarization coefficients for the incident P-wave and the homogenous waves induced at the interface,

$$u_x^{(m)} = \sqrt{\frac{\Gamma_{33}^{(m)} - \left(v_{1,2}^{(m)}\right)^2}{\Gamma_{11}^{(m)} + \Gamma_{33}^{(m)} - 2\left(v_{1,2}^{(m)}\right)^2}}, \tag{16}$$

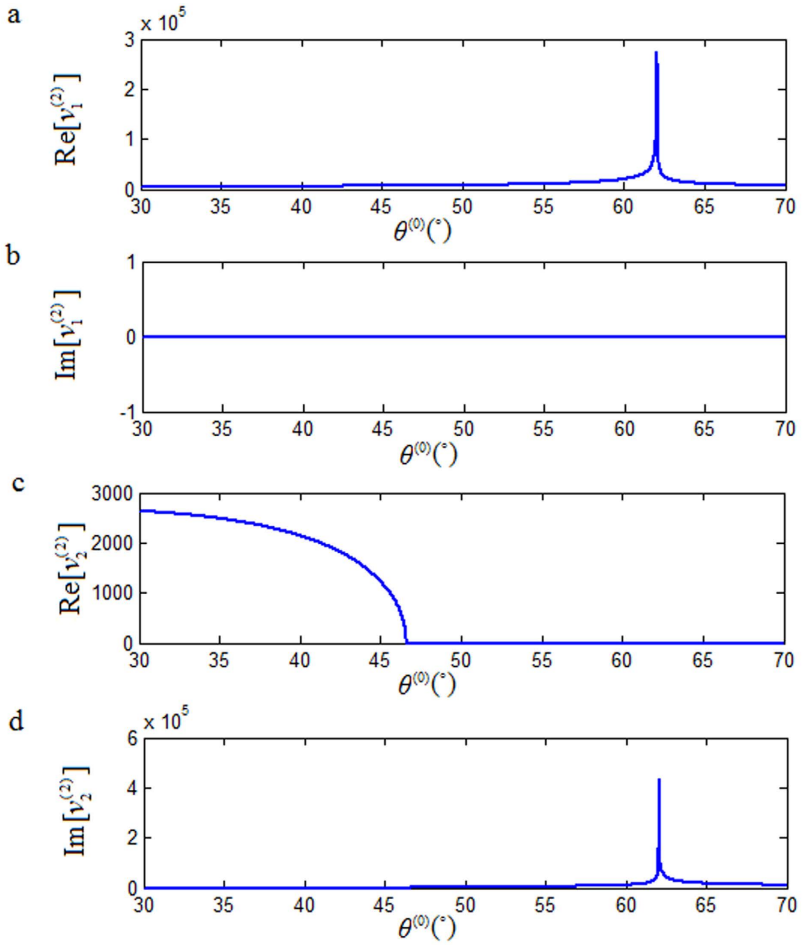

Figure 3. Relationships of both $v_1^{(2)}$ and $v_2^{(2)}$ versus $\theta^{(0)}$. a and b show that $v_1^{(2)}$ is purely real for $\theta^{(0)} \in [0°, 90°]$, and has a maximum at $\theta^{(0)} = 62.04°$; c and d show that $v_2^{(2)}$ is purely real for $\theta^{(0)} \in [0^\circ, 46.61^\circ]$ and is purely imaginary for $\theta^{(0)} \in [46.61^\circ, 90^\circ]$. The modulus of $v_2^{(2)}$ has a maximum at $\theta^{(0)} = 62.04°$.

$$u_z^{(m)} = \sqrt{\frac{\Gamma_{11}^{(m)} - (v^{(m)})^2}{\Gamma_{11}^{(m)} + \Gamma_{33}^{(m)} - 2(v^{(m)})^2}}, \tag{17}$$

For $\theta^{(0)} \in (\theta_c^{(2)}, 90^\circ)$ the refracted P-wave is inhomogenous. Eqs. (14) and (15) provide two sets of solutions for the polarization coefficients (refer to Eqs. (S9) and (S10) in "Supplementary material for Anomalous incident-angle and elliptical-polarization rotation of an elastically refracted P-wave").

$$u_x^{(2)} = \sqrt{\frac{\left|\Gamma_{13}^{(2)}\left(\Gamma_{33}^{(2)} - (v_1^{(2)})^2\right)\right|}{\left|(\Gamma_{13}^{(2)})^*\left(\Gamma_{33}^{(2)} - (v_1^{(2)})^2\right) + \Gamma_{13}^{(2)}\left(\Gamma_{11}^{(2)} - (v_1^{(2)})^2\right)\right|}}, \tag{18}$$

$$u_z^{(2)} = i\sqrt{\frac{\left|\Gamma_{13}^{(2)}\left(\Gamma_{11}^{(2)} - (v_1^{(2)})^2\right)\right|}{\left|(\Gamma_{13}^{(2)})^*\left(\Gamma_{33}^{(2)} - (v_1^{(2)})^2\right) + \Gamma_{13}^{(2)}\left(\Gamma_{11}^{(2)} - (v_1^{(2)})^2\right)\right|}}, \tag{19}$$

and

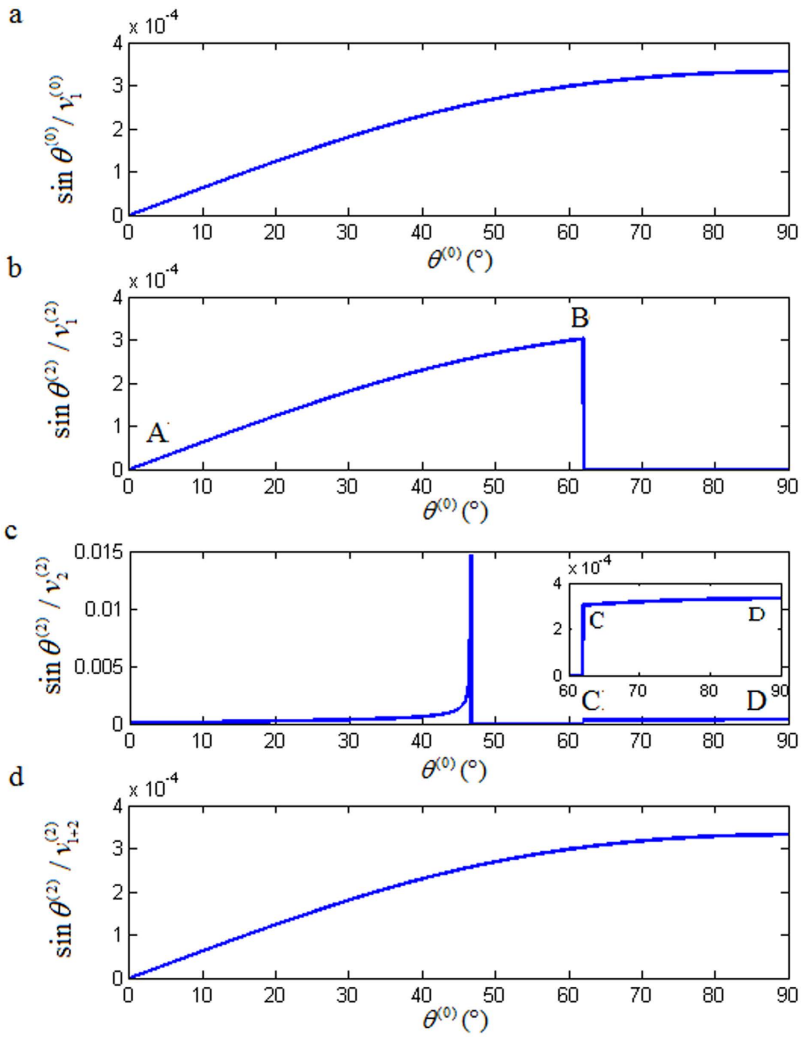

Figure 4. Relationships of sin $\theta^{(m)}/v_{1,2}^{(m)}$ versus $\theta^{(0)}$. $v_{1+2}^{(2)}$ stands for the phase velocity, $v_1^{(2)}$, of the refracted P-wave for $\theta^{(0)} \in [0°, 62.04°]$ and the phase velocity, $v_2^{(2)}$, of the refracted P-wave for $\theta^{(0)} \in [62.04°, 90°]$.

$$u_x^{(2)} = i\sqrt{\frac{\left|\Gamma_{13}^{(2)}\left(\Gamma_{33}^{(2)} - \left(v_1^{(2)}\right)^2\right)\right|}{\left|\left(\Gamma_{13}^{(2)}\right)^*\left(\Gamma_{33}^{(2)} - \left(v_1^{(2)}\right)^2\right) + \Gamma_{13}^{(2)}\left(\Gamma_{11}^{(2)} - \left(v_1^{(2)}\right)^2\right)\right|}}, \tag{20}$$

$$u_z^{(2)} = \sqrt{\frac{\left|\Gamma_{13}^{(2)}\left(\Gamma_{11}^{(2)} - \left(v_2^{(2)}\right)^2\right)\right|}{\left|\left(\Gamma_{13}^{(2)}\right)^*\left(\Gamma_{33}^{(2)} - \left(v_2^{(2)}\right)^2\right) + \Gamma_{13}^{(2)}\left(\Gamma_{11}^{(2)} - \left(v_2^{(2)}\right)^2\right)\right|}}. \tag{21}$$

An alternative confirmation of the anomalous incident-angle may be achieved by looking at the z-component of Poynting vector, which can be obtained from the reflection/refraction coefficients[11]. Specifically, we look at the normalized z-component, $P_z^{(0)}/\max(P_z^{(0)})$, of the incident P-wave. We also look at the normalized real parts of z-components from the four induced waves:

$$\boldsymbol{P}_z^{(sum)}/\max(\boldsymbol{P}_z^{(0)}) = \sum_{m=1}^{4} \mathrm{Re}(\boldsymbol{P}_z^{(m)})/\max(\boldsymbol{P}_z^{(0)}). \tag{22}$$

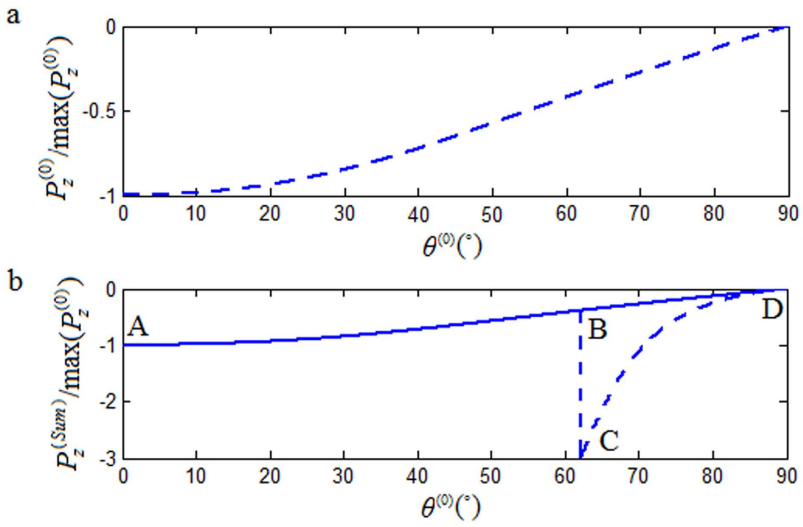

Figure 5. Relationships of $P_z^{(0)}/\max(P_z^{(0)})$ and $P_z^{(sum)}/\max(P_z^{(0)})$ versus $\theta^{(0)}$. (**b**) shows that the dashed-line segment $\overline{AB}$ stacks together with the solid-line segment $\overline{AB}$ for $\theta^{(0)} \in [0^\circ, \theta_a^{(2)}]$.

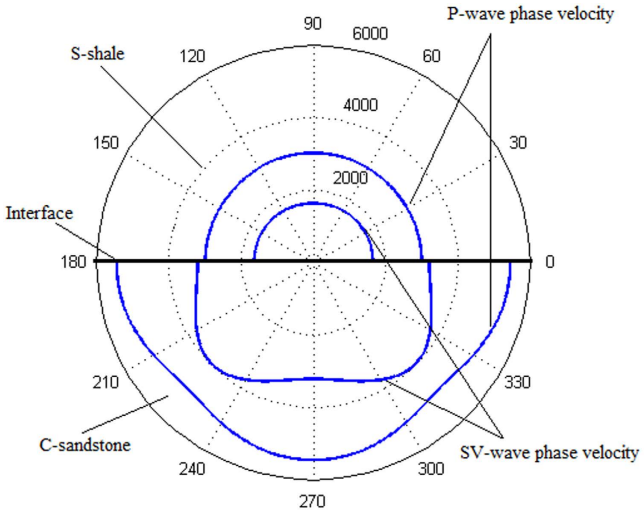

Figure 6. The calculated phase velocity curves for sandstone shale (S-shale) and calcareous sandstone (C-sandstone).

Now, consider the polarization coefficients calculated from Eqs. (16) and (17) as those of the incident P-wave, reflected P-wave, reflected SV-wave and refracted SV-wave for $\theta^{(0)} \in [0°, 90°]$ and the refracted P-wave for $\theta^{(0)} \in [0^\circ, \theta_c^{(2)}]$. Meanwhile, Eqs.(18) and (19) provide the polarization coefficients of the refracted P-wave for $\theta^{(0)} \in [\theta_c^{(2)}, 90^\circ]$. Then the normalized real parts of z-components of Poynting vectors are plotted dashed-lines in Fig. 5a,b. It shows clearly that, for $\theta^{(0)} \in [\theta_a^{(2)}, 90^\circ]$, the real part of $\boldsymbol{P}_z^{(sum)}$ is not identical to $\boldsymbol{P}_z^{(0)}$. Therefore, it is a violation of the energy balance principle. However, for $\theta^{(0)} \in [\theta_a^{(2)}, 90^\circ]$, if we switch the calculation of polarization coefficients from Eqs. (18) and (19) to Eqs. (20) and (21), then the real part of $P_z^{(sum)}$ is equal to $P_z^{(0)}$, as shown by the solid-line in Fig. 5b, which abides the energy balance principle.

For an inhomogenous refracted P-wave, the x-component of the polarization has a lag of 90° with respect to its z-component, which is defined as a left-rotational elliptical-polarized wave; otherwise, it is called a right-rotational elliptical-polarized wave. Figure 5 shows that a refracted P-wave is a linearly polarized wave for $\theta^{(0)} \in [0^\circ, \theta_c^{(2)}]$, a left-rotational elliptical-polarized wave for $\theta^{(0)} \in (\theta_c^{(2)}, \theta_a^{(2)})$, and a right-rotational elliptical-polarized wave for $\theta^{(0)} \in [\theta_a^{(2)}, 90^\circ]$. There is an elliptically-polarized rotational direction change at the anomalous incident-angle $\theta_a^{(2)} = 62.04^\circ$.

Discussion

The current studies of the interface between two VTI media show that there is an anomalous incident-angle $\theta_a^{(2)}$ with respect to the refracted P-wave in the area $\theta^{(0)} \in (\theta_c^{(2)}, 90^\circ)$. At such an incident-angle $\theta^{(0)} = \theta_a^{(2)}$, the phase velocity of the refracted P-wave must be switched from $\boldsymbol{v}_1^{(2)}$ to $\boldsymbol{v}_2^{(2)}$ to satisfy Snell's law. The inhomogeneously refracted P-wave experiences a sudden change from a left-rotational to a right-rotational elliptical-polarization.

It is worth noting that there is an anomalous incident-angle $\theta_a^{(2)}$ for the refracted P-wave, but no such an anomalous incident-angle $\theta^{(4)}$ for the refracted SV-wave. As an example, let's look at the interface between S-shale and C-sandstone. In this case, there are two critical incident-angles, i.e. $\theta_c^{(2)} = 33.41^\circ$ and $\theta_c^{(4)} = 70.66^\circ$. The phase velocity of P-waves in S-shale is smaller than those of P-waves and SV-waves in C-sandstone (see Fig. 6). There is an anomalous incident-angle corresponding to the refracted P-wave at $\theta_a^{(2)} = 46.19^\circ$. However, even with the second critical incident-angle $\theta_c^{(4)} = 70.66^\circ$ and the refracted SV-wave becoming an inhomogeneous wave for $\theta^{(0)} \in [\theta_c^{(4)}, 90^\circ]$, we have not observed the existence of an anomalous incident-angle $\theta_a^{(4)}$ corresponding to the refracted SV-wave.

References

1. Backus, G. L. Long-wave elastic anisotropy produced by horizontal layering. *J. Geophys. Res.* **67,** 4427–4440 (1962).
2. Thomsen, L. Weak elastic anisotropy. *Geophysics* **51,** 1954–1966 (1986).
3. Carcione, J. M. *Wave Fields in Real Media: Wave Propagation in Anisotropic, Anelastic and Porous Media* (Elsevier Science Vol. 31, Pergamon, 2001).
4. Ĉervenỳ, V. *Seismic Ray Theory* (Cambridge University Press, Cambridge, U. K., 2001).
5. Rüger, A. *Reflection Coefficients and Azimuthal AVO Analysis in Anisotropic Media* (Society of Exploration Geophysicists, No. 10, USA, 2002).
6. Auld, B. A. *Acoustic Fields and Waves in Solids* (Wiley Vol. 1, New York, USA, 1972).
7. Rüger, A. P-wave reflection coefficients for transversely isotropic models with vertical and horizontal axis of symmetry. *Geophysics* **62,** 713–722 (1997).
8. Daley, P. F. & Hron, F. Reflection and transmission coefficients for transversely isotropic media. *Bull. Seismol. Soc. Amer.* **67,** 661–675 (1977).
9. Crampin, S., Stephen, R. A. & McGonigle, R. The polarization of P-waves in anisotropic media. *Geophys. J. Roy. Astr. S.* **68,** 477–485 (1982).
10. Helbig, K. & Schoenberg, M. Anomalous polarization of elastic waves in transversely isotropic media. *J. Acoust. Soc. Am.* **81,** 1235–1245 (1987).
11. Fa, L., Brown, R. L. & Castagna, J. P. Anomalous post-critical refraction behavior for certain transversely isotropic media. *J. Acoust. Soc. Am.* **120,** 3479–3492 (2006).
12. Fa, L. *et al.* Polarization of plane wave propagating inside elastic hexagonal crystal solids. *Sci. China: Phys. Mech. Astron.* **57,** 263–272 (2014).
13. Nedimovic, M. R., Hyndman, R. D., Ramachandran K. & Spence, G. D. Reflection signature of seismic and aseismic slip on the northern Cascadia subduction interface. *Nature*. **424,** 416–420 (2003).
14. Canales, P., Nedimovic, M. R., Kent, G. M., Carbotte, S. M. & Detrick, R. S. Seismic reflection images of a near-axis sill within the lower crust at the Juan de Fuca ridge. *Nature*. **460,** 89–93 (2009).
15. Grady, N. K. *et al.* Terahertz metamaterials for linear polarization conversion and anomalous refraction. *Science*. **340,** 1304–1307 (2013).
16. Yu, N. *et al.* Light propagation with phase discontinuities: generalized laws of reflection and refraction. *Science*. **334,** 333–337 (2011).
17. Wang, Z. Seismic anisotropy in sedimentary rocks, part 2: Laboratory data. *Geophysics*. **67,** 1423–1440 (2002).

Acknowledgments

This work is supported by the National Natural Science Foundation of China (Grant No. 40974078) and by the Physical Sciences Division at The University of Chicago.

Author Contributions

L.F. and M.Z. initiated the project and contributed to the writing of the paper. Y.F. managed the project, Y.Z., P.D. and J.G. performed calculations, G.L. L.L. and S.T. checked calculated results. All authors co-wrote the paper.

Additional Information

Supplementary information accompanies this paper at http://www.nature.com/srep

Competing financial interests: The authors declare no competing financial interests.

How to cite this article: Fa, L. *et al.* Anomalous incident-angle and elliptical-polarization rotation of an elastically refracted P-wave. *Sci. Rep.* **5**, 12700; doi: 10.1038/srep12700 (2015).